Available online at www.sciencedirect.com
SCIENCE DIRECT®
Biochimica et Biophysica Acta 1608 (2004) 1–9
BIOCHIMICA ET BIOPHYSICA ACTA
BBA
www.bba-direct.com

Review

The gross structure of the respiratory complex I: a Lego System

Thorsten Friedrich[a,*], Bettina Böttcher[b]

[a] *Institut für Organische Chemie und Biochemie, Albert-Ludwigs-Universität Freiburg, Albertstr. 21, D-79104 Freiburg, Germany*
[b] *Structural and Computational Biology Programme, European Molecular Biology Laboratory, Meyerhofstr. 1, D-69117 Heidelberg, Germany*

Received 16 May 2003; received in revised form 26 September 2003; accepted 17 October 2003

Abstract

The proton-pumping NADH:ubiquinone oxidoreductase, also called complex I, is the entry point for electrons into the respiratory chains of many bacteria and mitochondria of most eucaryotes. It couples electron transfer with the translocation of protons across the membrane, thus providing the proton motive force essential for energy-consuming processes. Electron microscopy revealed the 'L'-shaped structure of the bacterial and mitochondrial complex with two arms arranged perpendicular to each other. Recently, we showed that the *Escherichia coli* complex I takes on another stable conformation with the two arms arranged side by side resulting in a horseshoe-shaped structure. This model reflects the evolution of complex I from pre-existing modules for electron transfer and proton translocation.

Keywords: NADH:ubiquinone oxidoreductase; Complex I; Electron microscopy; Single particle analysis; Image processing; Protein structure; Modular evolution

1. Introduction

The inner membrane of mitochondria and the cytoplasmic membrane of bacteria contain a proton-pumping NADH:ubiquinone oxidoreductase, which is also called respiratory complex I. Complex I is a multisubunit complex catalyzing the electron transfer from NADH to quinone coupled with the translocation of four protons across the membrane according to the equation:

$$NADH + Q + 5H_n^+ \rightarrow NAD^+ + QH_2 + 4H_p^+$$

where Q refers to quinone, and H_n^+ and H_p^+ to the protons taken up from the negative inner side and delivered to the positive outer side of the membrane [1–4]. In doing so, it contributes to the proton motive force required for energy-consuming processes. More recently, it has been demonstrated that in *Klebsiella pneumoniae* the complex translocates sodium ions instead of protons [5] and thus generates a sodium motive force. Homologues of complex I exist in the cyanobacteria, chloroplasts and archaea [6,7]. Characteristic features of complex I are its large number of subunits, its multiple prosthetic groups, namely one flavin mononucleotide (FMN) and up to nine iron–sulfur (Fe/S) clusters, and its sensitivity to a great variety of naturally occurring or synthetic inhibitors [8,9].

Due to its complex composition and the lack of high-resolution structural data, little is known about the mechanism of this large enzyme complex. However, it would be highly desirable to obtain more knowledge about the way complex I works in order to understand the molecular basis of a surely unique proton pump. In addition, it is now well-established that isolated complex I deficiencies are the most frequently encountered disturbances of the mitochondrial oxidative phosphorylation [10,11]. Finally, complex I is of industrial interest as a possible target for insecticides or acaricides [12,13].

This review will deal with the gross structure of complex I as revealed by electron microscopy. During the past years two-dimensional (2D) projection maps and three-dimensional (3D) structures of complex I from *Neurospora crassa* [14], *Escherichia coli* [15–17], *Bos taurus* [18,19], *Yarrowia lipolytica* [20,21], and *Aquifex aeolicus* [22] have been resolved at low resolution (17–34 Å). From the models derived by means of electron microscopy it is generally

Abbreviations: Complex I, proton-translocating NADH:ubiquinone oxidoreductase; Fe/S cluster, iron–sulfur cluster; FMN, flavin mononucleotide

* Corresponding author. Tel.: +49-761-203-6060; fax: +49-761-203-6096.
E-mail address: tfriedri@uni-freiburg.de (T. Friedrich).

0005-2728/$ - see front matter © 2003 Elsevier B.V. All rights reserved.
doi:10.1016/j.bbabio.2003.10.002

accepted that complex I has an L-shaped structure with two arms standing perpendicular to each other (for review see Ref. [23]). Recently, we have proposed that the *E. coli* complex I is capable of adopting another conformation with the two arms arranged side by side [17]. The significance of this observation as well as the modular structure of complex I will be discussed in this review.

2. Composition of complex I

The simplest form of a proton-pumping NADH:ubiquinone oxidoreductase known so far exists in bacteria [4–7,24]. In general, the bacterial complex consists of 14 different subunits, which add up to a molecular mass of about 535 kDa [25–28]. Homologues of these 14 subunits are part of complex I in all species known so far (Table 1). Therefore, it is suspected that they build the catalytic core of complex I and are called 'minimal' subunits [2,6]. The 14 different subunits are designated either as NuoA to NuoN or Nqo1 to Nqo14 in bacteria and can be classified in two groups (Table 1): seven subunits (NuoB–G and NuoI) are peripheral proteins including the subunits that bear all known redox groups of complex I. In addition, NuoF contains the NADH binding site [29] and NuoB and D are probably involved in quinone binding (Table 1) [30–32]. The remaining seven subunits (NuoA, H, and NuoJ–N) are mostly hydrophobic proteins predicted of folding into 54 α-helices across the membrane [6,7,24]. These subunits do not contain typical cofactor-binding motives and consequently no redox groups have been detected up to now. NuoH, L, and M are suspected of being involved in quinone binding [33–35]. As only the seven hydrophobic subunits are predicted of containing membrane-spanning helices, they are most likely also involved in proton translocation. This is supported by the fact that NuoL, M, N, and most likely NuoK are homologues to a distinct class of Na^+ (or K^+)/H^+ antiporter and are likely to contain H^+-pathways [7,24,36,37]. However, this assumption still awaits experimental verification.

In addition to the homologues of the 14 subunits present in bacteria, the mitochondrial complex I of eucaryotes contains at least 32 extra subunits resulting in a molecular mass of approximately 1 MDa [1,2,38]. The homologues of the seven hydrophobic subunits are mitochondrially encoded in eucaryotes. The extra subunits known so far are all encoded by nuclear genes [39]. Although their function is not clear, they probably form an insulation around complex I preventing the high energy electrons from escaping or they are needed to regulate the assembly of the complex [39]. However, at least four extra subunits seem to have a function specific for mitochondria: a 10 kDa subunit was found to be an acyl carrier protein with a phosphopantetheine as prosthetic group [40,41]. A 39/40 kDa "accessory" subunit contains a tightly bound NADPH and is related to short-chain dehydrogenases/reductases [42,43]. A 16.6 kDa subunit of bovine complex I was found to be GRIM-19, the product of a cell death regulatory gene [43]. Finally, an 18 kDa subunit is phosphorylated by a cAMP-dependent protein kinase and plays a role in the regulation of complex I activity [44].

Table 1
Nomenclature, localization and properties of the 14 'minimal' complex I subunits

Designation of subunit (Bacteria/Eucarya)	Localization	Predicted function
NuoA/ND3	membrane arm	?
NuoB/PSST	peripheral arm	[4Fe–4S]; N2 ubiquinone-binding?
NuoC/30 kDa (IP)[a]	peripheral arm	?
NuoD/49 kDa (IP)[a]	peripheral arm	Ubiquinone binding?
NuoE/24 kDa (FP)	peripheral arm	[2Fe–2S]; N1a
NuoF/51 kDa (FP)	peripheral arm	NADH- and FMN-binding [4Fe–4S]; N3
NuoG/75 kDa (IP)	peripheral arm	3 × [4Fe–4S]; N1c[b], N4, N5 [2Fe–2S], N1b
NuoH/ND1	membrane arm	Ubiquinone binding?
NuoI/TYKY	peripheral arm	2 × [4Fe–4S]; N6a, N6b
NuoJ/ND6	membrane arm	?
NuoK/ND4L	membrane arm	Proton translocation?
NuoL/ND5	membrane arm	Ubiquinone binding? Proton translocation?
NuoM/ND4	membrane arm	Ubiquinone binding? Proton translocation?
NuoN/ND2	membrane arm	Proton translocation?

[a] NuoC and D are fused in some bacteria.
[b] This cluster is only present in some bacteria.

3. The gross structure of complex I from bacteria and eucarya

The first structural information on complex I was derived from bovine heart complex I by means of single particle analysis and a tilt series of 2D membrane crystals [45,46]. The results were interpreted in a model showing four monomers arranged as a pair of dimers with a molecular mass of 1.6 MDa [46]. Later on, it turned out that the tetrameric crystals were composed of only a fragment of the complex [47]. Work carried out with the complex from *N. crassa* reconstituted in membranes revealed for the first time its two partite structure [47]. However, the derived model was not correct, due to an underestimation of the protein mass buried in the membrane. In a subsequent publication, the characteristic L-shape of the complex was described as being derived from single particle analysis and 2D membrane crystals [48]. One arm of the L, called the peripheral arm, protrudes into the aqueous phase and consists of the hydrophilic subunits. The other arm of the L, called the membrane arm, is embedded within the lipid bilayer and is made up of hydrophobic subunits (Fig. 1, Table 1). The two arms were distinguished from each other by electron micrographs of preparations of the individual arms of the *N. crassa* complex I [48].

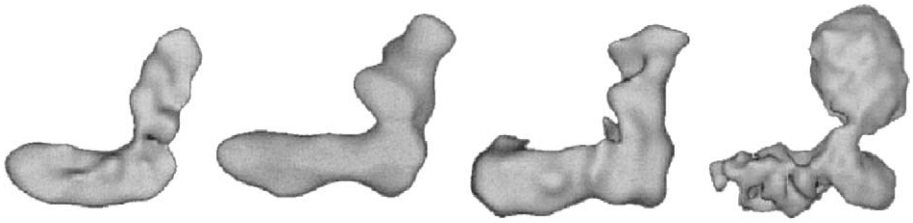

Fig. 1. Models of the 3D structures of complex I from *E. coli* [15], *Y. lipolytica* (M. Bostina, U. Brandt and M. Radermacher, personal communication), *N. crassa* [14] and *B. taurus* [18] (from left to right). A side-view is shown and the scale is identical for all views. The membrane arm runs horizontally. The model of the bovine complex I was derived by means of electron cryo-microscopy, the other models were derived from staining detergent solubilized complex I with uranyl acetate.

The more recent work on structure determination of complex I was done with single particle image analysis of negatively stained particles [14,15,17,18,21,22]. This technique has the advantage that no well-ordered 2D crystals are needed but is susceptible to artefacts caused by uneven staining of the particles or by flattening of the particles during drying. The detergent bound to the protein may affect the staining of the particle and variability of the individual particles may lead to a loss in resolution. Electron cryo-microscopy is often used to circumvent some of these problems, as the structure of the particles is preserved better, when surrounded by vitrified buffer [49]. Significant progress had been made along these lines with the bovine complex [18]. In addition, projection maps of 2D crystals of the bovine complex I have been obtained [19], however, 3D information on the organization of the complex within these crystals is still missing.

The models obtained from complex I from different sources all show the typical L-shaped structure (Fig. 1). The position of the peripheral arm of the *N. crassa* complex I was verified by immuno-labelling of the 49 kDa subunit, which is part of the peripheral arm [14]. The peripheral and membrane arms of the *E. coli* and *Y. lipolytica* complex I were attributed by alignment with the model of the *N. crassa* complex I [15,20]. Recently, this assignment was verified for *Y. lipolytica* by localizing the 49 kDa protein at a position comparable to the *N. crassa* complex [21]. The bovine complex was orientated relative to the membrane mainly by the mass distribution between the two arms and the presence of a constriction in one arm of the complex, which has also been detected in the membrane arm of the *N. crassa* complex I [14,18]. The two arms of the *A. aeolicus* complex have been assigned by similarity with the other models [22]. The models show that the two arms of the mitochondrial complex are about 23 nm and approximately of equal length [15,18]. More surprisingly, both arms of the bacterial complex are about 20 nm, thus being only slightly shorter than those of the mitochondrial complex, although the former contains only half the protein mass of the latter [15]. Comparison of the *N. crassa* complex with the *E. coli* complex suggests that the extra mass of the mitochondrial complex is evenly distributed around the catalytic core provided by the bacterial complex [15].

Although all models of complex I derived by means of electron microscopy show the same L-shaped structure, there are differences concerning details of the models (Fig. 1). Some of these variations may result from differences in the protein composition of the complexes, others from differences in staining or different approaches to image processing. A major question concerns the presence of a stalk connecting the two arms [18]. A stalk with a diameter of about 3 nm is present in the models of the bovine and *E. coli* complex I [15,18] but not in those of the *N. crassa* and *Y. lipolytica* enzyme ([14,48], M. Bostina, U. Brandt and M. Radermacher, personal communication). From a comparison of 3D maps of the *E. coli* and the *N. crassa* complex, Guénebaut et al. [15] concluded that in *N. crassa*, the stalk region might be filled with at least two additional subunits, which form a 50 kDa domain. This would lead to the conclusion that the stalk region is a genuine feature of the bacterial complex, which is filled by additional subunits in the mitochondrial complex I. However, the stalk may not be as thin as shown in Ref. [15] due to stain penetration. The bovine complex, which also has a stalk [18], does not fit into this picture. However, it is possible that some of the additional subunits in the stalk region are only loosely attached and could be lost or displaced during purification and concentration. On the other hand, it cannot be excluded that the stalk may represent a constriction in the membrane arm due to a wrong assignment of the arms in the 3D model.

Another difference concerns the angle between the two arms. A fixed angle of about 90° has been reported for the *N. crassa*, *B. taurus* and *A. aeolicus* complex [18,22,48], while this angle seems to be variable in the *E. coli* and *Y. lipolytica* complex ([15]; U. Brandt, personal communication). Values between 0° for the *E. coli* complex [17] and up to 180° for the *Y. lipolytica* complex (M. Bostina, U. Brandt and M. Radermacher, personal communication) have been reported. It is not known whether this has any significance for the mechanism of the complex (see below).

4. The alternative conformation of the *E. coli* complex I

The L-shaped structure of complex I is generally accepted [1–4]. However, the electron transport chain is spatially

separated from the membrane arm in this model (Fig. 2). The electron transfer from NADH to ubiquinone takes place solely in the peripheral arm, which comprises the binding sites for NADH, FMN and all FeS clusters [15]. Even the quinone-binding site is thought to be located in the connection between the peripheral and the membrane arm, because it is made up of hydrophilic as well as hydrophobic subunits [3,6,24,33,50].

The membrane arm, constituting approximately half of the protein mass, is involved in quinone binding and in proton translocation (Table 1; [24,32–36,51]). Mutations in all subunits of the membrane arm reduce the electron transport activity of complex I ([52,53], http://www.mitomap.org.) leading to the conclusion that proton translocation in the membrane arm must be coupled with the electron transfer in the peripheral arm. The spatial separation of the coupled events of electron transport and proton transport led many groups to the proposal of an indirect mechanism of proton pumping which is driven by conformational changes [54–56]. This proposal is supported by several experiments: (1) the labelling pattern of complex I by either photoaffinity inhibitors or cross-linkers depends on the redox state of the complex [57–59]. (2) Amiloride-type inhibitors, which were originally described as inhibitors of Na^+/H^+ antiporters, are found to act specifically on complex I [33,60,61]. As it is thought that antiporters operate by conformational changes, a similar mechanism is anticipated for complex I [55]. (3) It is supposed that that the subunits NuoL and M which are most likely involved in proton translocation are located at the distal end of the membrane arm spatially separated from the redox groups in the peripheral arm [19,62]. (4) FT-IR spectroscopy has directly shown that the redox reaction of complex I is accompanied by large protein rearrangements [63–65].

A mechanism of complex I including conformational changes was also supported by the finding that the *K. pneumoniae* complex I translocates sodium ions instead of protons [5]. The translocation of sodium ions can hardly be imagined by a direct pumping mechanism. However, it was also reported that this enzyme works with a stoichiometry of 2 Na^+ per 2 e^- [5], while 4 H^+ per 2 e^- have been determined for the proton translocating complex I from bacteria and mitochondria [66–71]. The high sequence identity between the proton pumping *E. coli* complex I [69,71] and the sodium pumping *K. pneumoniae* complex I [5] makes it unlikely that they operate with completely different mechanisms. It was suggested that complex I contains two coupling sites, one employing direct redox coupling with the Fe/S cluster N2 and the other involving an indirect, conformationally linked type of mechanism (Fig. 2; [54]). This assumption agrees well with the hypothesis that complex I evolved from pre-existing blocks for electron transport and proton translocation ([7,24,36,37]; and see below). The lower ion per electron stoichiometry of the sodium pumping enzyme may be due to the activity of only the conformationally linked coupling site.

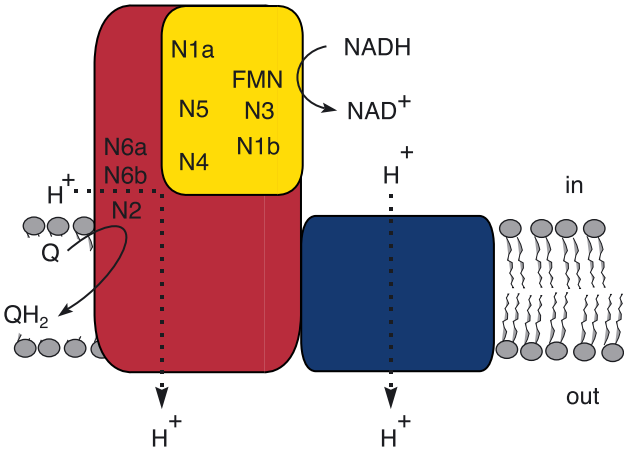

Fig. 2. Cartoon of complex I, showing the three modules. The NADH dehydrogenase module is drawn in yellow, the hydrogenase module in red and the transporter module in blue. The Fe/S clusters are denoted as N1a, N1b, N2, N3, N4, N5, N6a, and N6b. The two proposed coupling sites are indicated, see text for details.

A conformationally coupled mechanism of complex I implies a major movement of the protein as demonstrated for the F-type ATP-synthases or P-type-ATPases. Thus, one would expect at least two different conformations of complex I. Recently, we demonstrated that in *E. coli*, the L-shaped conformation is only one of at least two stable conformations of the isolated complex [17]. In the other conformation, the peripheral and the membrane arm are arranged parallel to each other (Fig. 3). In vitro, the transition between the two conformations is induced by the ionic strength of the buffer and is completely reversible. At high ionic strength, the L-shaped conformation is observed. At low ionic strength, the complex takes an alternative conformation with both arms arranged side by side as in a horseshoe [17]. It is noteworthy that the conformational change is apparently due to a movement of the electron input module of the complex. In the L-shaped conformation, this module is buried within the peripheral arm and it is opened out in the horseshoe-shaped conformation representing a separate peripheral domain. In the horseshoe-shaped conformation, each of the two arms is formed by two distinct domains (Fig. 3). Annotation of the two arms of the complex was made by comparison with a fragment of the complex lacking the peripheral electron input module (Fig. 3; [6,7,17]). This approach identified one of the two peripheral domains as the electron input module. We propose that the individual domains display the different modules from which complex I emerged during evolution (see below).

Our studies have recently been challenged by a report by Sazanov et al. [16] demonstrating that the isolated *E. coli* complex I is in the L-shaped conformation in 2D crystals and that this conformation is enzymatically active. The horseshoe-shaped conformation was not detected in this study. The differences between this and our study seem to be due to the different purification protocols resulting in

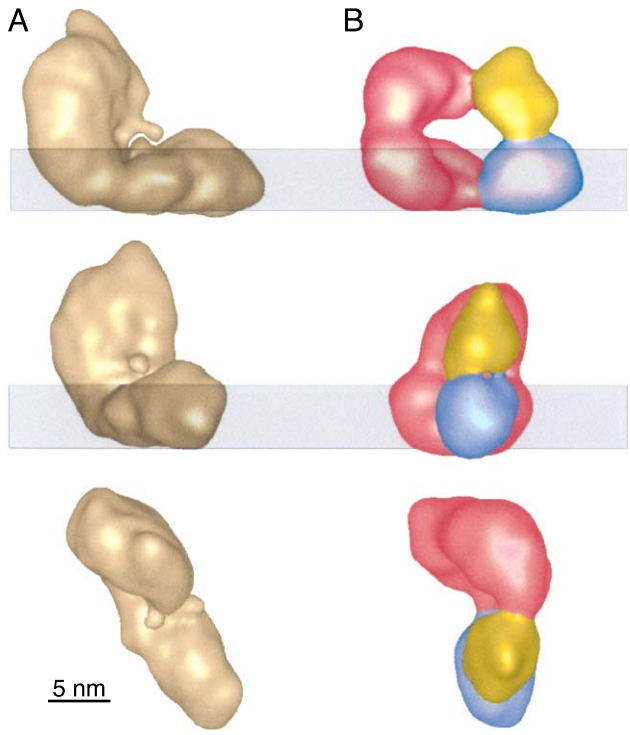

Fig. 3. Model of *E. coli* complex I conformations in a buffer of high (A) and low (B) ionic strength. The first and the second row show orthogonal views of surface representations parallel to the plane of the membrane. The third row views normal to the plane of the membrane. The bilayer is symbolized by the grey shaded area. The NADH dehydrogenase module is drawn in yellow, the hydrogenase module in red and the transporter module in blue. The scale is given.

subtle but probably important differences in the isolated complex. These differences most likely concern the phospholipid and quinone content of both preparations. Many properties of membranous protein complexes are influenced by the amount of lipid bound to the preparation [72]. Our preparation contains 0.5 mol ubiquinone per mole of complex I and approximately five lipid molecules per molecule of complex I ([34]; T. Friedrich, unpublished data). Most likely due to the low amount of lipids contained in the preparation, the enzyme exhibits very little activity in detergent solution, which is stimulated 20-fold by an addition of *E. coli* lipids. The preparation described by Sazanov et al. shows four times as much activity in detergent solution than our preparation but is only activated 3-fold by an addition of phospholipids under comparable experimental conditions (approximately 100 mM salt, added *E. coli* polar lipids dissolved in dodecyl maltoside) [16]. Accordingly, the lipid-stimulated activity in both preparations is comparable. However, only the activity of our preparation is sensitive to rotenone and piericidin A [17,71], which is indicative of a physiological decyl–ubiquinone reduction [73,74]. Another difference is the presence of $CaCl_2$ in the Sazanov protocol. Due to this, a certain amount of $CaCl_2$ is carried over with the protein to all assays. It is shown that the presence of these ions stabilizes the complex [16], probably by fixing it in a certain, i.e. L-shaped conformation. This hypothesis is supported by the formation of 2D crystals of complex I in the presence of $CaCl_2$, where the conformational homogeneity of the complex would be beneficial.

The suggestion that the horseshoe-shaped conformation is only a result of a dimerization of the membrane arm of the *E. coli* complex I [16] can be completely ruled out for three reasons: first, analytical ultracentrifugation has unambiguously shown that our preparation has an identical molecular mass with the same number of components in a buffer of high and low ionic strength. Merely the sedimentation coefficient changes from 22 S in a buffer of low ionic strength to 15 S in a buffer of high ionic strength [17]. These observations are consistent with a conformational change but not with a disintegration/dimerization event. Secondly, neither the dimer of the membrane arm nor the residual peripheral arm show inhibitor-sensitive NADH:quinone reductase activity which we measured for the horseshoe-shaped conformation. Thirdly, the change from the horseshoe-shaped conformation to the L-shaped conformation accompanied by a loss of activity is completely reversible.

This leaves the question: which conformation type occurs in the lipid bilayer at more physiological salt concentrations? Information on this issue comes from the analysis of complex I reconstituted in a membrane in 2D crystals. Different groups have reported side-view projections at the edge of the complex which are consistent with the L-shape [16,48]. Unfortunately, the length of the peripheral arm of the complex protruding from the lipid bilayer in side-views of the 2D crystals is an ambiguous criterion to distinguish between the L- or the horseshoe-shaped conformation as the difference in height is only minor [17] and insignificant at the given uncertainty of orientation. Conclusions on the conformational state of the complex were also drawn from 2D projection maps of the crystals, which are in agreement with the peripheral arm projecting out of the membrane as expected in the L-shaped conformation. Interestingly, depending on the crystal packing, a smaller density at the distal end of the membrane arm was observed for the *E. coli* complex, which was not present in the single molecule representations [16]. It has been argued that this distal density is solely caused by a different penetration of the stain in the different crystal forms [16]. However, the observation of the smaller density at the distal end would also agree with a horseshoe-shaped conformation, because the constriction in the peripheral arm would lead to two distinct densities in projection. Of these two densities, the distal one corresponding to a smaller mass should also be smaller (Fig. 4, insert). Without a 3D map, it will be impossible to decide which conformation the complex has in this type of crystal.

We took a different approach for information on the conformational state of the *E. coli* complex I in the membrane. The complex was reconstituted in liposomes of *E. coli* polar lipids (protein/lipid 1:4 (w/w) in 50 mM MES/NaOH, 50 mM NaCl, pH 6.0 as described in Ref. [75]) and

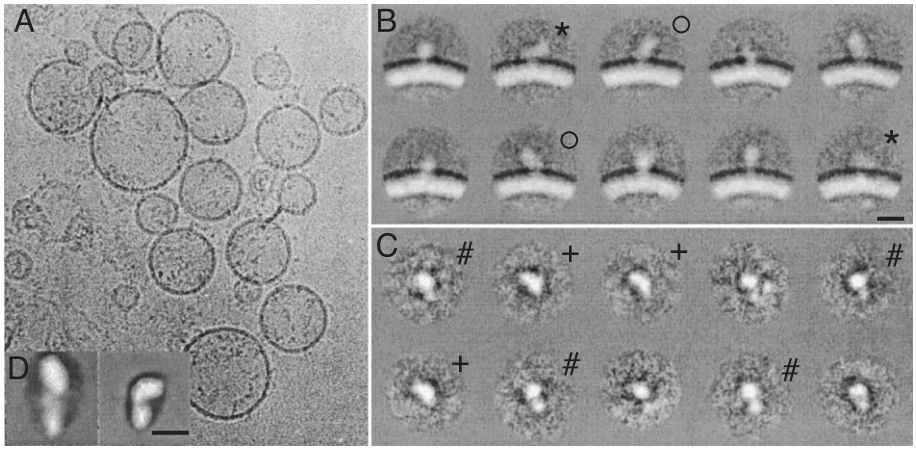

Fig. 4. *E. coli* complex I reconstituted in phospholipids. (A) Micrograph of proteoliposomes embedded in vitrified buffer. (B) Class averages of 380 side-view projections of complex I. Projections with the peripheral arm parallel to the surface of the liposomes as expected for the horseshoe-shaped conformation are marked with (*), intermediate orientations are marked with (○). (C) Class averages of 260 top view projections. Some of the projections show a larger slightly elongated density (+) as expected for L-shaped particles, others show a larger and a smaller density (#) as expected for horseshoe-shaped particles. (D) Calculated top view projections of the L-shaped (left) and horseshoe-shaped complex (right) as published in Ref. [17]. The scale bar marks 100 Å.

embedded in vitrified buffer at normal salt concentrations (50 mM MES/NaOH, 50 mM NaCl, pH 6.0; Fig. 4). In liposomes, the complex has no conformational constraints like those caused by the packing of the protein in a 2D crystal. Therefore, the complex can adopt any stable conformation. To understand the resulting projection maps, some basic geometrical considerations have to be taken: in general, at the edge of the liposomes, side-view projections parallel to the plane of the membrane are observed, whereas in the centre of the liposomes, top-view projections perpendicular to the plane of membrane are found. In a first approximation, an L-shaped particle should show only one type of side-view projection, with the peripheral arm seen as a rod-like feature perpendicular to the membrane. For a horseshoe-shaped particle, a similar side-view projection is expected although protruding slightly less. Therefore, the observation of rod-shaped projections perpendicular to the membrane are not evidence for the presence or absence of an L- or horseshoe-shaped conformation. For the horseshoe-shaped conformation, there should also be other side-view projections where the peripheral arm is approximately parallel to the surface of the liposome. Such side-views were indeed observed (Fig. 4B (*)) and could not be explained by the presence of L-shaped particles alone. The occurrence of these particles required a conformation in which the membrane arm is more or less parallel to the plane of membrane as for example in the horseshoe-shaped conformation. However, it is still impossible to distinguish between a conformation in which the peripheral arm is parallel to the membrane arm or in which there is an angle close to 180° between membrane arm and peripheral arm.

In a conformationally homogeneous population, top-view projections should all be similar and should be related by in-plane rotation and/or mirror symmetry. We observed not one but two types of top-views in liposomes (Fig. 4C (#) and (+)). These projections were similar to calculated projections of the 3D map of the horseshoe-shaped and L-shaped complexes (Fig. 4D; [17]). From these observations, we conclude that the *E. coli* complex I reconstituted in liposomes can adopt different conformations, which vary in the position of the peripheral arm and are in principle consistent with an L-shaped and a horseshoe-shaped conformation. From this, we propose that the peripheral arm of the complex has some conformational flexibility and might perform small movements similar to a handle of a pump during catalysis. The horseshoe-shaped conformation and the conformation with a 180° angle between the two arms (see above) might reflect two extreme positions of this conformational flexibility.

5. The modular structure of complex I

Sequence analysis revealed that complex I evolved from three major modules for electron transport and proton translocation [6,7,24,36,37,54]. The soluble NADH dehydrogenase module represents the electron input part mentioned above. This module is also found in many non-energy-converting NAD(P)H-dependent hydrogenases and dehydrogenases and is involved in electron transfer [6,7]. The hydrogenase module is made up of hydrophilic as well as hydrophobic subunits and is also present in a family of membrane-bound multisubunit [NiFe] hydrogenases [76]. This module is involved in redox-coupled proton translocation [54,76]. The transporter module is entirely formed by hydrophobic subunits, among them homologues of H^+/Na^+ or H^+/K^+ antiporter subunits [36,37,51], indicating their possible involvement in conformational-driven ion-translocation in complex I [54].

The modular evolution of the complex is reflected in its Lego-like structure (Fig. 3B). The model of the 3D structure of complex I at low ionic strength shows the presence of

four distinct domains in a defined spatial relation to each other [17]. The position of the NADH dehydrogenase module is obvious from the comparison of the model of a fragment of complex I missing this module [17]. As depicted in Fig. 3B, it corresponds to the yellow domain in the upper right position. This module is linked to the hydrogenase module, thus connecting the electron transport chain from NADH to ubiquinone [54]. The hydrogenase module corresponds to the two domains on the left side of the model drawn in red in Fig. 3B. The upper domain corresponds to the hydrophilic subunits of this module, while the lower one is made up of the hydrophobic subunits. The transporter module is attached to the membranous domain of the hydrogenase module. The connection between these two hydrophobic domains is visible as a constriction detected in the membrane arm of the *N. crassa* and the bovine complex I [18,19,48]. In the horseshoe-shaped conformation derived from negatively stained single particles, the transporter module seems to have contact with the NADH dehydrogenase module (Fig. 3B). The modular evolution of complex I was first recognized from the conserved gene order of the complex I genes in bacteria and the homology of these genes to other genes coding for different enzymes [6]. Now, the modular evolution of the complex is seen in its modular overall structure as well. The modules with different functions for electron transfer and proton translocation were combined during evolution like bricks from a Lego System.

Acknowledgements

Work from the authors' laboratories was supported by the Deutsche Forschungsgemeinschaft and the Fonds der Chemischen Industrie. We are grateful to Linda Böhm for her help in preparing the manuscript.

References

[1] H. Weiss, T. Friedrich, G. Hofhaus, D. Preis, The respiratory-chain NADH dehydrogenase (complex I) of mitochondria, Eur. J. Biochem. 197 (1991) 563–576.
[2] J.E. Walker, The NADH:ubiquinone oxidoreductase (complex I) of respiratory chains, Q. Rev. Biophys. 25 (1992) 253–324.
[3] U. Brandt, Proton-translocation by membrane-bound NADH:ubiquinone-oxidoreductase (complex I) through redox-gated ligand conduction, Biochim. Biophys. Acta 1318 (1997) 79–91.
[4] T. Yagi, The bacterial energy-transducing NADH–quinone oxidoreductases, Biochim. Biophys. Acta 1141 (1993) 1–17.
[5] A.C. Gemperli, P. Dimroth, J. Steuber, Sodium ion cycling mediates energy coupling between complex I and ATP synthase, Proc. Natl. Acad. Sci. U. S. A. 100 (2003) 839–844.
[6] T. Friedrich, K. Steinmüller, H. Weiss, The proton-pumping respiratory complex I of bacteria and mitochondria and its homologue in chloroplasts, FEBS Lett. 367 (1995) 107–111.
[7] T. Friedrich, D. Scheide, The respiratory complex I of Bacteria, Archaea, and Eucarya and its module common with membrane-bound multisubunit hydrogenases, FEBS Lett. 479 (2000) 1–5.
[8] M. Degli Esposti, Inhibitors of NADH–ubiquinone reductase: an overview, Biochim. Biophys. Acta 1364 (1998) 222–236.
[9] H. Miyoshi, Structure–activity relationships of some complex I inhibitors, Biochim. Biophys. Acta 1364 (1998) 236–245.
[10] J. Smeitink, R. Sengers, F. Trijbels, L. van den Heuvel, Human NADH:ubiquinone oxidoreductase, J. Bioenerg. Biomembranes 33 (2001) 259–266.
[11] R. Janssen, J. Smeitink, R. Smeets, L. van den Heuvel, CIA30 complex I assembly factor: a candidate for human complex I deficiency? Hum. Genet. 110 (2002) 264–270.
[12] P.J. Jewess, A.L. Devonshire, Kinetic microplate-based assays for inhibitors of mitochondrial NADH:ubiquinone oxidoreductase (complex I) and succinate:cytochrome *c* oxidoreductase, Anal. Biochem. 272 (1999) 56–63.
[13] P. Lümmen, Biochemical aspects of N-heterocyclic complex-I inhibitors with insecticidal activity, Biochem. Soc. Trans. 27 (1999) 602–606.
[14] V. Guénebaut, R. Vincentelli, D. Mills, H. Weiss, K.R. Leonard, Three-dimensional structure of NADH-dehydrogenase from *Neurospora crassa* by electron microscopy and conical tilt reconstruction, J. Mol. Biol. 265 (1997) 409–418.
[15] V. Guénebaut, A. Schlitt, H. Weiss, K.R. Leonard, T. Friedrich, Consistent structure between bacterial and mitochondrial NADH:ubiquinone oxidoreductase (complex I), J. Mol. Biol. 276 (1998) 105–112.
[16] L.A. Sazanov, J. Carroll, P. Holt, L. Toime, I.M. Fearnley, A role for native lipids in the stabilization and two-dimensional crystallization of the *Escherichia coli* NADH:ubiquinone oxidoreductase (complex I), J. Biol. Chem. 278 (2003) 19483–19491.
[17] B. Böttcher, D. Scheide, M. Hesterberg, L. Nagel-Steger, T. Friedrich, A novel, enzymatically active conformation of the *Escherichia coli* NADH:ubiquinone oxidoreductase (complex I), J. Biol. Chem. 277 (2002) 17970–17977.
[18] N. Grigorieff, Three-dimensional structure of bovine NADH:ubiquinone oxidoreductase (complex I) at 22 Å in ice, J. Mol. Biol. 277 (1998) 1033–1046.
[19] L.A. Sazanov, J.E. Walker, Cryo-electron crystallography of two subcomplexes of bovine complex I reveals the relationship between the membrane and peripheral arms, J. Mol. Biol. 302 (2000) 455–464.
[20] R. Djafarzadeh, S. Kerscher, K. Zwicker, M. Radermacher, M. Lindahl, H. Schägger, U. Brandt, Biophysical and structural characterization of proton-translocating NADH-dehydrogenase (complex I) from the strictly aerobic yeast *Yarrowia lipolytica*, Biochim. Biophys. Acta 1459 (2000) 230–238.
[21] V. Zickermann, M. Bostina, C. Hunte, T. Ruiz, M. Radermacher, U. Brandt, Functional Implications from an unexpected position of the 49 kDa subunit of NADH:ubiquinone oxidoreductase, J. Biol. Chem. 278 (2003) 29072–29078.
[22] G. Peng, G. Fritzsch, V. Zickermann, H. Schägger, R. Mentele, F. Lottspeich, M. Bostina, M. Radermacher, R. Huber, K.O. Stetter, H. Michel, Isolation, characterization and electron microscopic single particle analysis of the NADH:ubiquinone oxidoreductase (complex I) from the hyperthermophilic eubacterium *Aquifex aeolicus*, Biochemistry 42 (2003) 3032–3039.
[23] N. Grigorieff, Structure of the respiratory NADH:ubiquinone oxidoreductase (complex I), Curr. Opin. Struck. Biol. 9 (1999) 476–483.
[24] T. Friedrich, H. Weiss, Modular evolution of the respiratory NADH:ubiquinone oxidoreductase and the origin of its modules, J. Theor. Biol. 187 (1997) 529–541.
[25] T. Yagi, T. Yano, A. Matsuno-Yagi, Characteristics of the energy-transducing NADH–quinone oxidoreductase of *Paracoccus denitrificans* as revealed by biochemical, biophysical, and molecular biological approaches, J. Bioenerg. Biomembranes 25 (1993) 339–345.
[26] T. Yano, S.S. Chu, V.D. Sled', T. Ohnishi, T. Yagi, The proton-translocating NADH–quinone oxidoreductase (NDH-1) of thermophilic bacterium *Thermus thermophilus* HB-8. Complete DNA sequence of the gene cluster and thermostable properties of the expressed NQO2 subunit, J. Biol. Chem. 272 (1997) 4201–4211.

[27] U. Weidner, S. Geier, A. Ptock, T. Friedrich, H. Leif, H. Weiss, The gene locus of the proton-translocating NADH:ubiquinone oxidoreductase in *Escherichia coli*. Organization of the 14 genes and relationship between the derived proteins and subunits of the mitochondrial complex I, J. Mol. Biol. 233 (1993) 109–122.
[28] A. Dupuis, M. Chevallet, E. Darrouzet, H. Duborjal, J. Lunardi, J.P. Issartel, The complex I from *Rhodobacter capsulatus*, Biochim. Biophys. Acta 1364 (1998) 147–169.
[29] W. Fecke, V.D. Sled', T. Ohnishi, H. Weiss, Disruption of the gene encoding the NADH-binding subunit of NADH:ubiquinone oxidoreductase in *Neurospora crassa*. Formation of a partially assembled enzyme without FMN and the iron–sulphur cluster N-3, Eur. J. Biochem. 220 (1994) 551–558.
[30] I. Prieur, J.L. Lunardi, A. Dupuis, Evidence for a quinone binding site close to the interface between NUOD and NUOB subunits of complex I, Biochim. Biophys. Acta 1504 (2001) 173–178.
[31] F. Schuler, T. Yano, S. DiBernardo, T. Yagi, V. Yankovskaya, T. Singer, J.E. Casida, NADH–quinone oxidoreductase: PSST subunit couples electron transfer from iron–sulfur cluster N2 to quinone, Proc. Natl. Acad. Sci. U. S. A. 96 (1999) 4149–4153.
[32] F. Schuler, J.E. Casida, Functional coupling of PSST and ND1 subunits in NADH:ubiquinone oxidoreductase established by photoaffinity labeling, Biochim. Biophys. Acta 1506 (2001) 79–87.
[33] S. Kerscher, N. Kashani-Poor, K. Zwicker, V. Zickermann, U. Brandt, Exploring the catalytic core of complex I by *Yarrowia lipolytica* yeast genetics, J. Bioenerg. Biomembranes 33 (2001) 187–196.
[34] E. Nakamaru-Ogiso, K. Sakamoto, A. Matsuno-Yagi, H. Miyoshi, T. Yagi, The ND5 subunit was labeled by a photoaffinity analogue of fenpyroximate in bovine mitochondrial complex I, Biochemistry 42 (2003) 746–754.
[35] X. Gong, T. Xie, L. Yu, M. Hesterberg, D. Scheide, T. Friedrich, C.A. Yu, The ubiquinone-binding site in NADH:ubiquinone reductase from *Escherichia coli*, J. Biol. Chem. 278 (2003) 25731–25737.
[36] C. Mathiesen, C. Hagerhall, Transmembrane topology of the NuoL, M and N subunits of NADH:quinone oxidoreductase and their homologues among membrane-bound hydrogenases and bona fide antiporters, Biochim. Biophys. Acta 1556 (2002) 121–132.
[37] C. Mathiesen, C. Hagerhall, The 'antiporter module' of respiratory chain complex I includes the MrpC/NuoK subunit—a revision of the modular evolution scheme, FEBS Lett. 549 (2003) 7–13.
[38] J. Hirst, J. Carroll, I.M. Fearnley, R.J. Shannon, J.E. Walker, The nuclear encoded subunits of complex I from bovine heart mitochondria, Biochim. Biophys. Acta 1604 (2003) 135–150.
[39] J. Carroll, I.M. Fearnley, R.J. Shannon, J. Hirst, J.E. Walker, Analysis of the subunit composition of complex I from bovine heart mitochondria, Mol. Cell. Proteomics 2 (2003) 117–126.
[40] U. Sackmann, R. Zensen, D. Röhlen, U. Jahnke, H. Weiss, The acyl-carrier protein in *Neurospora crassa* mitochondria is a subunit of NADH:ubiquinone reductase (complex I), Eur. J. Biochem. 200 (1991) 463–469.
[41] M.J. Runswick, I.M. Fearnley, J.M. Skehel, J.E. Walker, Presence of an acyl carrier protein in NADH:ubiquinone oxidoreductase from bovine heart mitochondria, FEBS Lett. 286 (1991) 121–124.
[42] U. Schulte, V. Haupt, A. Abelmann, W. Fecke, B. Brors, T. Rasmussen, T. Friedrich, H. Weiss, A reductase/isomerase subunit of mitochondrial NADH:ubiquinone oxidoreductase (complex I) carries an NADPH and is involved in the biogenesis of the complex, J. Mol. Biol. 292 (1999) 569–580.
[43] I.M. Fearnley, J. Carrol, R.J. Shannon, M.J. Runswick, J.E. Walker, J. Hirst, GRIM-19, a cell death regulatory gene product, is a subunit of bovine mitochondrial NADH:ubiquinone oxidoreductase (complex I), J. Biol. Chem. 276 (2001) 38345–38348.
[44] S. Papa, A.M. Sardanelli, S. Scacco, V. Petruzzella, Z. Technikova-Dobrova, R. Vergari, A. Signorile, The NADH:ubiquinone oxidoreductase (complex I) of the mammalian respiratory chain and the cAMP cascade, J. Bioenerg. Biomembranes 34 (2002) 1–10.
[45] E.J. Boekema, J.F.L. van Breemen, W. Keegstra, E.F.J. van Bruggen, S.P.J. Albracht, Structure of NADH:Q oxidoreductase from bovine heart mitochondria studied by electron microscopy, Biochim. Biophys. Acta 679 (1982) 7–11.
[46] E.J. Boekma, M.G. van Heel, E.F.J. van Bruggen, Three-dimensional structure of bovine NADH:ubiquinone oxidoreductase of the mitochondrial respiratory chain, Biochim. Biophys. Acta 787 (1984) 19–26.
[47] K.R. Leonard, H. Haiker, H. Weiss, Three-dimensional structure of NADH:ubiquinone reductase (complex I) from *Neurospora* mitochondria determined by electron microscopy of membrane crystals, J. Mol. Biol. 194 (1987) 277–286.
[48] G. Hofhaus, H. Weiss, K.R. Leonard, Electron microscopic analysis of the peripheral and membrane parts of mitochondrial NADH dehydrogenase (complex I), J. Mol. Biol. 221 (1991) 1027–1043.
[49] J. Dubochet, M. Adrian, J.J. Chang, J.C. Homo, J. Lepault, A. McDowall, P. Schultz, Cryo-electron microscopy of vitrified specimens, Q. Rev. Biophys. 21 (1988) 129–228.
[50] N. Kashani-Poor, K. Zwicker, S. Kerscher, U. Brandt, A central functional role for the 49-kDa subunit within the catalytic core of mitochondrial complex I, J. Biol. Chem. 276 (2001) 24082–24087.
[51] A.A. Guffanti, Y. Wei, S.V. Rood, T. Krulwich, An antiport mechanism for a member of the cation diffusion facilitator family: divalent cations efflux in exchange for K^+ and H^+, Mol. Microbiol. 45 (2002) 145–153.
[52] B.H. Robinson, Human complex I deficiency: clinical spectrum and involvement of oxygen free radicals in the pathogenicity of the defect, Biochim. Biophys. Acta 1364 (1998) 271–286.
[53] A.H.V. Schapira, Mitochondrial dysfunction in neurodegenerative disorders, Biochim. Biophys. Acta 1364 (1998) 261–270.
[54] T. Friedrich, Complex I: a chimaera of redox and conformation driven proton-pump? J. Bioenerg. Biomembranes 33 (2001) 169–178.
[55] T. Yagi, A. Matsuno-Yagi, The proton-translocating NADH–quinone oxidoreductase in the respiratory chain: the secret unlocked, Biochemistry 42 (2003) 2266–2274.
[56] U. Brandt, S. Kerscher, S. Dröse, K. Zwicker, V. Zickermann, Proton pumping by NADH:ubiquinone oxidoreductase. A redox driven conformational change mechanism? FEBS Lett. 545 (2003) 9–17.
[57] J.A. Gondal, W.M. Anderson, The molecular morphology of bovine heart mitochondrial NADH–ubiquinone reductase. Cross-linking with dithiobis(succinimidyl propionate), J. Biol. Chem. 260 (1985) 12690–12694.
[58] G.I. Belogrudov, Y. Hatefi, Catalytic sector of complex I (NADH:ubiquinone oxidoreductase): subunit stoichiometry and substrate-induced conformation changes, Biochemistry 33 (1994) 4571–4576.
[59] M. Yamaguchi, G.I. Belogrudov, Y. Hatefi, Mitochondrial NADH–ubiquinone oxidoreductase (Complex I). Effect of substrates on the fragmentation of subunits by trypsin, J. Biol. Chem. 273 (1998) 8094–8098.
[60] J. Steuber, The C-terminally truncated NuoL subunit (ND5 homologue) of the Na^+-dependent complex I from *Escherichia coli* transports Na^+, J. Biol. Chem. 278 (2003) 26817–26822.
[61] E. Nakamaru-Ogiso, B.B. Seo, T. Yagi, A. Matsuno-Yagi, Amiloride inhibition of the proton-translocating NADH–quinone oxidoreductase of mammals and bacteria, FEBS Lett. 549 (2003) 43–46.
[62] P.J. Holt, D.J. Morgan, L.A. Sazanov, The location of NuoL and NuoM subunits in the membrane domain of the *Escherichia coli* complex I: implications for the mechanism of proton pumping, J. Biol. Chem. 278 (2003) 43114–43120.
[63] P. Hellwig, D. Scheide, S. Bungert, W. Mäntele, T. Friedrich, FT-IR spectroscopic characterization of NADH:ubiquinone oxidoreductase (complex I) from *Escherichia coli*: oxidation of FeS cluster N2 is coupled with the protonation of an aspartate or glutamate side chain, Biochemistry 39 (2000) 10884–10891.
[64] D. Flemming, P. Hellwig, T. Friedrich, Involvement of tyrosines 114 and 139 of subunit NuoB in the proton pathway around cluster N2 in *Escherichia coli* NADH:ubiquinone oxidoreductase, J. Biol. Chem. 278 (2003) 3055–3062.

[65] P. Hellwig, S. Stolpe, T. Friedrich, FTIR spectroscopic study on the conformational reorganisation in *E. coli* complex I due to redox-driven proton translocation, Biospectroscopy (in press).
[66] M. Wikström, Two protons are pumped from the mitochondrial matrix per electron transferred between NADH and ubiquinone, FEBS Lett. 169 (1984) 300–304.
[67] C.G. Brown, M.D. Brand, Proton/electron stoichiometry of mitochondrial complex I estimated from the equilibrium thermodynamic force ratio, Biochem. J. 252 (1988) 473–479.
[68] P.C. Hinkle, M.A. Kumar, A. Resetar, D.L. Harris, Mechanistic stoichiometry of mitochondrial oxidative phosphorylation, Biochemistry 30 (1991) 3576–3582.
[69] A.V. Bogachev, R.A. Murtazina, V.P. Skulachev, H^+/e^- stoichiometry for NADH dehydrogenase I and dimethyl sulfoxide reductase in anaerobically grown *Escherichia coli* cells, J. Bacteriol. 178 (1996) 6233–6237.
[70] A.S. Galkin, V.G. Grivennikova, A.D. Vinogradov, $H^+/2e^-$ stoichiometry of the NADH:ubiquinone reductase reaction catalyzed by submitochondrial particles, Biochemistry (Mosc.) 66 (2001) 435–443.
[71] S. Stolpe, T. Friedrich, The *Escherichia coli* NADH:ubiquinone oxidoreductase (complex I) is a primary proton-pump capable of secondary sodium antiport (submitted for publication).
[72] C. Lange, J.H. Nett, B.L. Trumpower, C. Hunte, Specific roles of protein–phospholipid interactions in the yeast cytochrome *bc*1 complex structure, EMBO J. 20 (2001) 6591–6600.
[73] F. Di Virgilio, G.F. Azzone, Activation of site I redox-driven H^+ pump by exogenous quinones in intact mitochondria, J. Biol. Chem. 257 (1982) 4106–4113.
[74] E. Estornell, R. Fato, F. Pallotti, G. Lenaz, Assay conditions for the mitochondrial NADH:coenzyme Q oxidoreductase, FEBS Lett. 332 (1993) 127–131.
[75] J.L. Rigaud, G. Mosser, J.J. Lacapere, A. Olofsson, D. Levy, J.L. Ranck, Bio-Beads: an efficient strategy for two-dimensional crystallization of membrane proteins, J. Struct. Biol. 118 (1997) 226–235.
[76] A. Teerstegen, R. Hedderich, *Methanobacterium thermoautotrophicum* encodes two multisubunit membrane-bound [NiFe] hydrogenases. Transcription of the operons and sequence analysis of the deduced proteins, Eur. J. Biochem. 264 (1999) 930–943.